AVO estimation using surface-related multiple prediction

Stewart A. Levin, Mobil Upstream Strategic Research Center*

Summary

In this work I explore the use of surface-related multiple prediction in enhancing AVO estimation. Multiple reflections from a proposed reflection event are predicted using surface-related multiple generation (Verschuur et al., 1988) and compared to the actual data to identify anomalous amplitude behavior. Synthetic elastic point source data is used to illustrate this approach.

Introduction

Surface-related multiple attenuation is derived from a surface-related multiple feedback equation

$$U=(1-U)R \tag{1}$$

which expresses the fact that the recorded data U is the sum of the direct illumination of the subsurface R and the secondary illumination with the reflected data $-U$. (A more precise formulation is given by, e.g., Wang and Levin, 1994.) In particular, the surface multiples in our data are given by the term $-UR$. Each primary reflection, P, in R produces the multiple train $-UP$.

Suppose we now generate a synthetic primary reflection, P_0 , with constant amplitude that matches the moveout of an actual event in our data. Assuming our data is relative-amplitude compensated (divergence corrections and cable balancing are applied), the AVO response of the multiple prediction $-UP_0$ should match the AVO of the multiples in the actual data just as the AVO response of the primary P_0 should match the AVO of the actual primary it models. If there are systematic deviations, we conclude that we are seeing an AVO effect.

This strategy offers some potentially nice features:

- It is an incremental improvement to conventional AVO. The additional information given by multiples may enhance and stabilize AVO estimation from multiple-contaminated data.
- The approach relies only on relative amplitudes along events. The absolute scaling may change from one arrival to another. Unlike multiple attenuation, I do not seek to match absolute amplitudes.
- Since multiple reflections amplify small time differences, a later multiple may separate from a strong, interfering event, allowing AVO estimation to proceed unhampered.

Because the angular aperture of later arrivals is smaller, the angular resolution of AVO measurements from multiple reflections is higher.

1-D

The surface-related multiple prediction works on prestack data from a 2-D line. In the special case of a horizontally-layered earth, the process reduces to a 2-D convolution of a representative shot record with the proposed primary event. This is equivalent to multiplying their *F-K* transforms together, making investigation of the process exceptionally easy without losing the generality of the full prestack prediction.

Let us look at a synthetic example. Figure 1 is an elastic synthetic seismogram generated for a point source over a 1-D earth model. This model was developed from well logs. Using the interactive *Overlay* program (Claerbout, 1987), I picked the seafloor reflector and generated a flat, constant-amplitude event with the same zero-offset intercept. Filtering to the frequency range of the synthetic and inverse NMO application produced the template in Figure 2. Convolving there together produces the surface multiple train in Figure 3. With the exception of some aliased energy and finite-aperture artifacts, the predicted multiples align well with the multiples in the data. The phase differences are due to the half derivative implicit in two-dimensional hyperbolic summation being applied to data generated in three dimensions.

Correlating offsets

The ability to model relative amplitudes along multiple reflection events is not useful unless we can correlate the amplitude changes to specific offsets, or at least offset ranges, of the corresponding primary reflection. The way I've chosen to approach

this problem is to emulate a "beam" by applying bell-shaped weights centered around specific offsets on the model primary. By inserting this smoothly-peaked function into the process, I generate a template of multiple arrivals associated with this offset. Figures 4 and 5 show sample bell-weighted primaries and Figures 6 and 7 show the corresponding multiple event templates they generate. You can clearly see the constant-slope peaks moving approximately radially. This amplifies the point made in the introduction: later arrivals have less angular aperture and more angular resolution. Furthermore, the aliasing artifacts from Figure 3, which arise from the steep, aliased portion of the hyperbola in Figure 2, are no longer present.

AVO Estimation

In the previous sections we have seen that multiples can be predicted and offsets can be correlated between primary and multiple arrivals. Now I turn to AVO estimation using these tools. Three strategies come to mind, which I order according to what stage the user needs to pick amplitudes:

1. Apply a conventional AVO measurement procedure to the multiple-contaminated data and use the offset correlations to combine primary and multiple AVO.
2. Use the multiple template to decide where to pick amplitudes and use the offset correlations to combine primary and multiple AVO.
3. Combine the offset-restricted multiples with the input dataset, by, say, normalized cross-correlation, and pick a suitable peak as the AVO measurement.

Strategy 1 is severely hampered by the fact that multiples generally do not flatten at primary velocity, but AVO is measured along constant time slices. It will be necessary to perform velocity scans on the predicted multiples for each separate primary reflection of interest. This is essentially strategy 2 — use the multiple template to tell us where to pick amplitudes on the multiple-contaminated data. My initial attempts to implement strategy 2 did not succeed due to bugs and limitations in the local seismic processing system's ability to apply the needed NMO velocity profile to flatten the multiples for AVO picking.

Strategy 3 avoids direct amplitude picking and relies on being able to emulate multiples well enough so that amplitude variations with offset are dominated by artifacts of the emulation algorithm. A fit of the offset-limited multiple panels to the input data then provides AVO estimates.

Least-squares fitting

My approach to strategy 3 is illustrated in Figures 8 through 10. The offset axis is broken into a series of partially overlapping ranges from which a sequence of multiple models, M_1 to M_n, are generated. A least-squares problem is then set up

$$U \approx \sum a_j \; M_j \tag{2}$$

to estimate AVO coefficients a_j . Dividing through by the first coefficient produces an amplitude versus offset curve from the multiple template. I use a weighted least-squares approach in order to accommodate divergence, and possibly other, corrections.

In more detail:

1. The input data are scaled by $t^{½}$ to emulate 2-D divergence.
2. A primary reflection is identified with the *Overlay* program.
3. A constant-amplitude model is
   - generated at the primary reflection time,
   - bandpass filtered,
   - inverse NMO'ed with the primary velocity, and
   - scaled by $t^{-½}$ to emulate 2-D divergence

   to produce a primary template.
4. The offset range is divided into approximately equal, partially-overlapping pieces.
5. For each offset segment:
   - The constant amplitude model is bell-tapered for that segment. The tapers are renormalized so that they sum to 1 between the first and last bell centers.
   - The range-limited primary synthetic is suitably convolved with the input data to emulate multiples.

- The multiple template is rho-filtered to correct for 3-D to 2-D phase differences.

6. The suite of offset-limited panels and the input data are scaled by $t^{1/2}$ as partial preconditioning.
7. The reciprocal envelope of the input data is computed and muted to just prior to the arrival of the first multiple. These weights are used for preconditioning of the least-squares (Verschuur et al., 1988).
8. *Not yet implemented:* Each multiple panel is cross-correlated with the input data to estimate and apply a small residual alignment filter.
9. A least-squares fit is done to estimate the AVO coefficients a_j in equation (2).

Applying this procedure to the data over the offset range 0-1800 meters produces the AVO estimation of Figure 12. Picking the largest amplitude sample at the corresponding offsets on the primary event yields Figure 11. While we can see that both graphs have the same general trend, peaking around offset 600-800 m., the multiple estimates jump around a good deal more. Blinking between the multiple template and the input data shows the probable cause of the instability — a progressive timing shift between early and late multiples. This reflects the sensitivity of multiples to small timing differences. In this case my zero-offset intercept time looks to be about 4 ms. too large for the model primary. Future work to appear in the SEG presentation will address this.

Conclusions

The illustrations and examples in this work show how AVO effects are produced and modeled on multiple reflections and suggest one way in which they may be used to improve the reliability and resolution of AVO measurement.

References

Claerbout, J.F., 1987, Interpretation with the *Overlay* program: Stanford Expl. Proj. Report 51, 269-300.

Verschuur, D.J., Hermann, P., Kinneging, N.A., Wapenaar, C.P.A., and Berkhout, A.J., 1988, Elimination of surface-related multiply reflected and converted waves: 58th Annual Internat. Mtg., Soc. Expl. Geophys., Expanded Abstracts, 1017-1020.

Wang, Y., and Levin, S.A., 1994, An investigation into eliminating surface multiples: Stanford Expl. Proj. Report 80, 589-602.

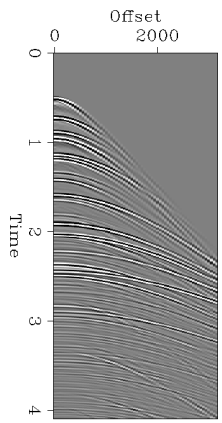

Fig 1. Synthetic elastic seismogram generated by Haskell-Thompson modelling.

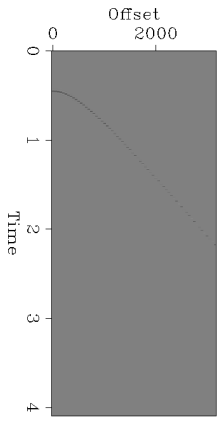

Fig 2. Constant-amplitude model of water bottom reflection.

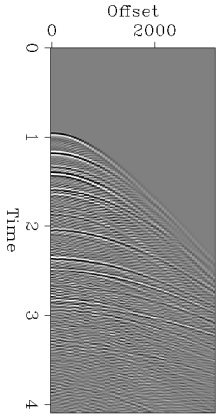

Fig 3. Water bottom multiple train predicted by convolving the datasets in Figs 1 and 2.

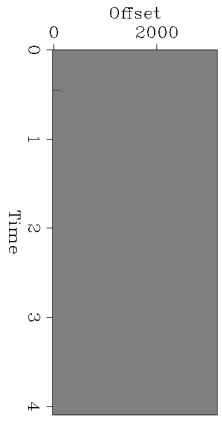

Fig 4. Model of water bottom reflection bell-tapered around zero offset.

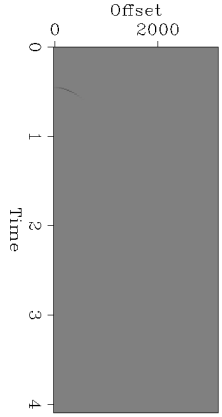

Fig 5. Model of water bottom reflection bell-tapered around an offset of 750 m.

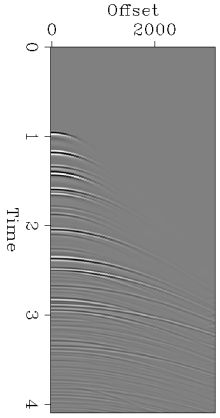

Fig 6. Multiple template of zero-offset multiples.

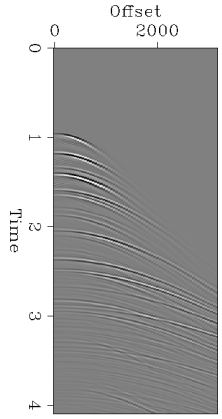

Fig 7. Multiple template of near-offset multiples.

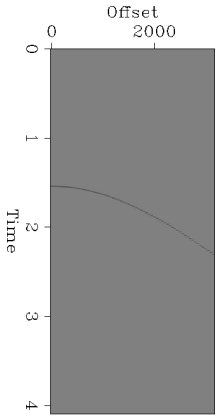

Fig 8. Model of deeper reflector at 1.5552 sec.

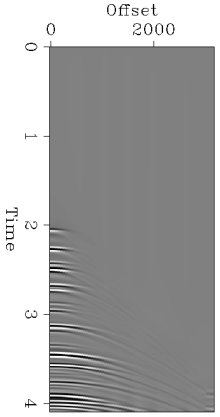

Fig 9. Multiple model for zero-offset of deeper reflector.

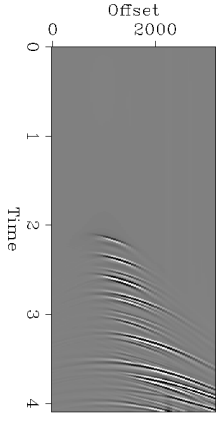

Fig 10. Multiple model for intermediate offset of deeper reflector.

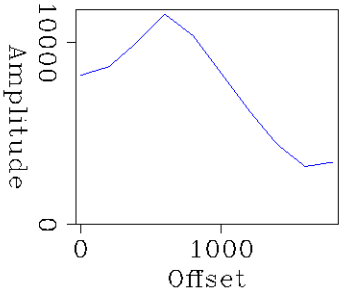

Fig 11. Relative amplitudes picked from primary reflection.

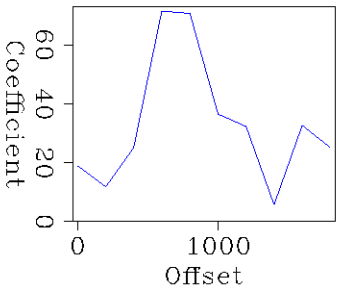

Fig 12. Relative amplitudes estimated from multiples.